

Superparamagnetic behavior of ZnFe₂O₄ nanoparticles as evidenced by EPR

O. RAITA, A.POPA*, D.TOLOMAN, V.BADILITA^a, R. R. PITICESCU^a, L.M.GIURGIU

*National Institute for Research and Development of Isotopic and Molecular Technologies
400293 Cluj-Napoca, P. O. Box 700, Romania*

^aNational R&D Institute for Nonferrous and Rare Metals, 102 Biruintei Blvd., Pantelimon, Ilfov, Romania

We report the investigation by electron paramagnetic resonance (EPR) in X and Q- bands of the nature of magnetic interactions present in ZnFe₂O₄ nanoparticles. EPR spectrum consists of a single broad line. In the investigated temperature range and both bands, the resonance field shifts to lower fields and the line broadens with the decrease of temperature. These features are the signature for the presence of a superparamagnetic state in ZnFe₂O₄. From magnetic measurements, a superparamagnetic behavior for ZnFe₂O₄ powders was confirmed.

(Received January 8, 2015; accepted September 9, 2015)

Keywords: electron paramagnetic resonance, spinel, magnetic behavior, nanoparticles

1. Introduction

As an important member of the ferrites family, zinc ferrite (ZnFe₂O₄) receives scientific attention due to its interesting magnetic behavior which depends on the particle size [1, 2]. It belongs to a class of normal spinels, MFe₂O₄, with a tetrahedral (A) site occupied by Zn²⁺ ions and Fe³⁺ ions occupying octahedral (B) site [3]. It is known that ZnFe₂O₄ has paramagnetic properties at room temperature and long range antiferromagnetic order below Néel temperature of about 10 K [4]. Its paramagnetic behavior could be due to the occurrence of the negative superexchange interactions between Fe³⁺ ions [5].

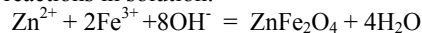
Recently, depending on the synthesis procedure, a possible ferromagnetic behavior at high temperatures was evidenced in ZnFe₂O₄ powders, thin films and nanoparticles [6 –9]. There are quite a few reports concerning the characterization of the ferromagnetic state in different ZnFe₂O₄ compounds by electron paramagnetic resonance (EPR) [10 – 12].

The investigations of the magnetic properties of diluted magnetic semiconductors such as Fe- doped ZnO, reveal the importance of the secondary phases, such as ZnFe₂O₄, for the magnetic ordering in these systems [13, 14]. The presence of this impurity phase could be attributed to the heat treatment of the samples during the synthesis procedure. The evidence of ferromagnetism in Fe- and Cu- codoped samples was proved to be associated with the formation of nonstoichiometric spinel ferrite phases [15]. FMR investigations of Fe- doped ZnO systems confirm the presence of Fe³⁺ ions [16, 17]. There are two possible sources of Fe³⁺ ions: (i) the vacancies in the nearest neighborhood of the doped Fe²⁺ ions can convert the valence state of Fe to +3 and (ii) Fe³⁺ ions from the ZnFe₂O₄ impurity spinel phase, if it is present in the system.

In this paper we study the magnetic behavior of zinc ferrite nanoparticles. The temperature dependences of the EPR line width and resonance field in X and Q- bands were investigated. The obtained results could be important for a correct assignment of the Fe³⁺ resonances in Fe-doped magnetic semiconductors.

2. Experimental

ZnFe₂O₄ nanoparticles were synthesized as follows. Inorganic precursors of zinc nitrate tetrahydrate (Zn(NO₃)₂·4H₂O Merck) and iron (III) chloride hexahydrate (FeCl₃·6H₂O) (Merck) were used in the synthesis. Firstly an aqueous solution was obtained by dissolution in distilled water under stirring. The pH of the solution was then adjusted at pH 9.5-10.0 by addition of ammonia, based on calculation of OH⁻ ions required for the reactions in solution:



The final precipitate was filtered, washed with water distilled three times to eliminate soluble impurities and dried in an oven. The chemical composition was analyzed by Direct Coupled Plasma Spectrometry (DSC-Spectroflame) showing that no impurities with content higher than 0.1% were detected in the spinel powder.

Structural characterization by X-ray diffraction (XRD) was performed on Bruker D8 Advance diffractometer using CuK α radiation, the Diffrac^{plus} XRD Commander (Bruker AXS) software, the Bragg-Brentano diffraction method and ICDD PDF-2 Release 2006 database.

Scanning electron microscopy (SEM) analysis was carried out with a JEOL JSM 5510 LV, with EDX; Resolution: 3,5 nm; accelerating voltage: 100 kV; magnification: 300.000 x .

Electron paramagnetic resonance (EPR) measurements of the powder samples were performed on a Bruker ELEXSYS 500 spectrometer operating at X-band (9.52 GHz) and Q-band (34.08 GHz) frequencies. The following experimental arrangements were used: microwave power, 2 mW; modulation frequency, 100 kHz; magnetic field modulation amplitude; 10 G. The spectra were measured in the temperature range of 120–300 K using a variable temperature accessory and the processing was performed by Bruker Xepr software. The EPR spectra were recorded using equal quantities of samples.

The magnetic measurements in function of temperature were performed by using a Vibrating Sample Magnetometer (VSM) DMS 880.

3. Results and discussion

X-ray powder diffraction (XRD) was used to analyze the structural properties and to identify the phase and the purity of the sample. Fig. 1 presents the X-ray powder diffraction pattern recorded for the ZnFe₂O₄ sample. One can see a typical diffraction pattern of the spinel which crystallized in a cubic system corresponding to the space group Fd-3m (227). The observed well defined diffraction peaks corresponding to the (311), (511) and (440) characteristic planes appear at $2\theta = 35.2^\circ$, 56.5° and 62° , respectively.

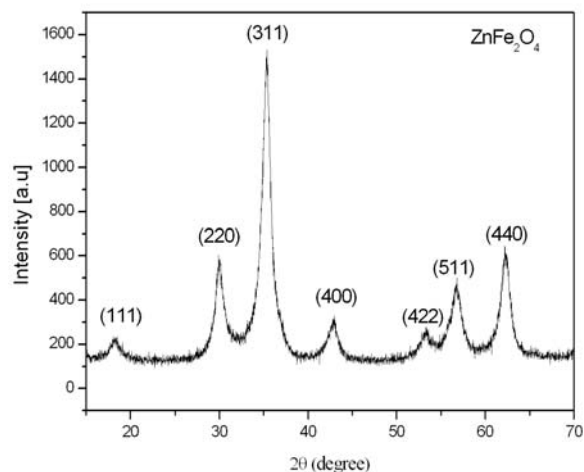


Fig. 1 XRD diffraction pattern of ZnFe₂O₄ sample.

These peaks match with the database ICDD 70-6393 (released 2006) and are very similar with the data published in the literature [6, 18]. Mean crystallite size calculated from X-ray line broadening using the Scherrer formula is about 6.5 nm. No additional peaks expect that for ZnFe₂O₄ were observed, thus indicating that the sample is free of impurity phases.

The particles' size and morphology were characterized by SEM microscopy. The image of ZnFe₂O₄ nanoparticles is shown in Fig. 2. It was observed that the individual particles have almost spherical shape with a mean size of 18 nm. However an inherent agglomeration of the individual particles was also noticed.

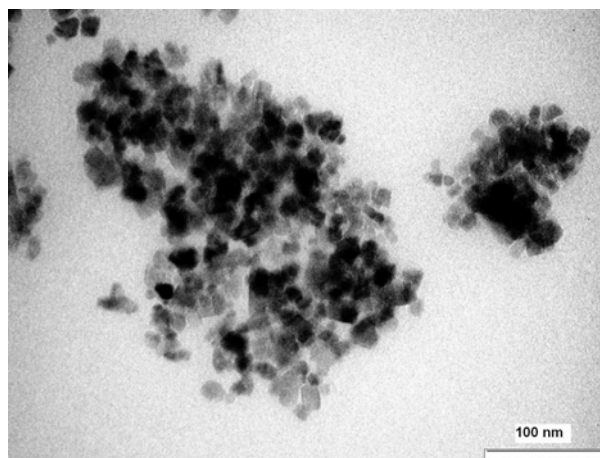


Fig. 2 SEM image of ZnFe₂O₄ nanoparticles.

In order to better understand the magnetic behavior of the nanoparticles, VSM measurements were performed. The magnetization curves versus applied field, measured at different temperatures are shown in Fig. 3. The obtained curves does not show hysteresis loop, being typical for superparamagnetic behavior. Taking into account that the nanoparticles mean size is about 18 nm this behavior was expected.

To get information about the spin-dynamics of nanosized system, the EPR spectra were recorded in the temperature range of 120K- 300K, in both X and Q – bands. EPR spectroscopy is a powerful tool to study through the changes in the temperature dependences of the resonance field and line width of spectra, the nature of the magnetic interactions present in a system, the range of magnetic ordering, magnetic inhomogeneity, spin fluctuations, etc. [16].

In the investigated temperature range, the EPR spectrum for ZnFe₂O₄ nanoparticles consists of a single quite broad line. Figures 4a and 4b show typical EPR spectra of ZnFe₂O₄ recorded at two different temperatures in X and Q - bands. The observed signal could be attributed to the resonance arising from exchange interactions between the Fe³⁺ ions. In order to characterize the degree of the asymmetry of the observed lines, we have introduced the asymmetry parameter A/B. Here, the A and B values are the amplitudes of the low and high field wings of the resonance line, respectively. Our measurements show that the lines have a slightly asymmetrical line shape, $A/B \approx 1.2$, in both bands and in the entire temperature range.

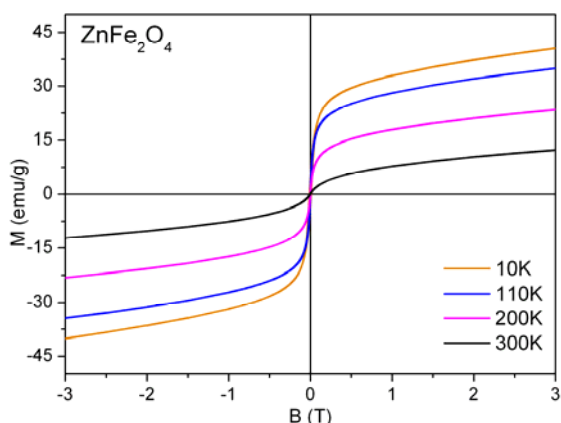


Fig. 3 Hysteresis curves measured at different temperatures.

An inspection of the Fig. 4 shows that there is a line broadening and a shift of the magnetic field position of the line to the lower field in both bands as the temperature is lowered. Such temperature dependent changes in the field position and line width of the resonance occur in the superparamagnetic state [21].

In Fig. 5 we have represented the shift of the resonance field, ΔH_R , (i.e., the difference between the observed resonance field and the center of the resonance of isolated Fe^{3+} ions, $g \approx 2$) at X and Q - bands as function of temperature for ZnFe_2O_4 nanoparticles. As expected, these plots clearly illustrate a gradual shift of the center of the resonance to lower fields with the lowering of the temperature. ΔH_R gradually decreases with the increase in the temperature and probably it vanishes for higher temperatures above 300 K. As one can see from Fig. 5, there is a dependence of ΔH_R on the experimental frequency for our ZnFe_2O_4 nanoparticles.

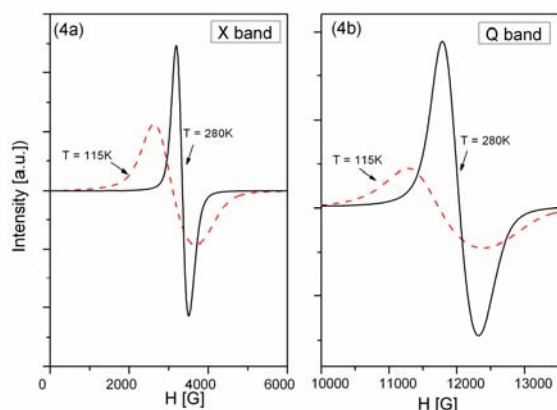


Fig. 4 EPR line in X-band (a) and Q-band (b) at two different temperatures: $T=115$ K (dashed line) and $T=280$ K (solid line) for ZnFe_2O_4 nanoparticles.

In principle there are two causes which could explain the shift of the resonance to lower fields [22]. The first possibility implies the interspin interactions which in the magnetically concentrated systems, lead to an increase in the g factor. For our case:

$$g_{\text{eff}} = g_{\text{Fe}} + \Delta g \quad (1)$$

where Δg is the change in the g factor induced by the spin fluctuations. In this approach the resonance field, H_R , and the corresponding shift, ΔH_R , are related by [22]:

$$H_R \approx \frac{hf}{g_{\text{Fe}}\mu_B} - \frac{hf\Delta g}{g_{\text{Fe}}^2\mu_B} = \frac{hf}{g_{\text{Fe}}\mu_B} + \Delta H_R \quad (2)$$

Here, h is the Planck constant, f is the frequency, $g_{\text{Fe}} = 2.0$ and μ_B is the Bohr magneton. If the cause for the observed shift is the change in the g factor (Eq. 2), then the resonance shift, ΔH_R , will increase with the experimental frequency.

The second scenario takes into account the fact that the shift could arise because the spins feel a field, H_{eff} , which is different from the applied field:

$$H_{\text{eff}} = H_{\text{appl}} + H_{\text{int}} \quad (3)$$

Here, H_{int} is a local field at the Fe^{3+} site due to the surrounding spin sublattice and the resonance is observed at H_{appl} which is expressed by [22].

$$H_R = \frac{hf}{g_{\text{Fe}}\mu_B} - H_{\text{int}} \quad \Delta H_R = H_{\text{int}} \quad (4)$$

If ΔH_R originates from an internal field, then it will remain approximately constant as function of the frequency.

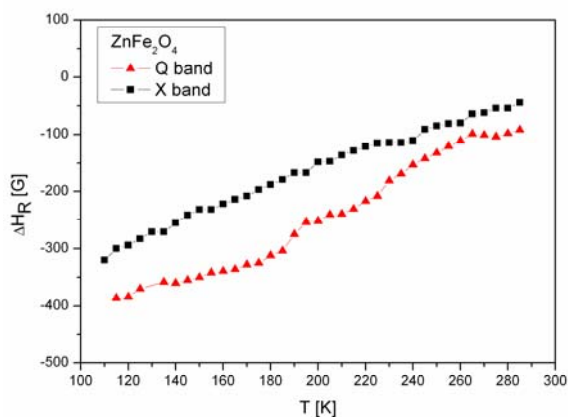


Fig. 5 Shift of the resonance field, ΔH_R , as function of temperature observed in X and Q bands.

The data for ZnFe₂O₄ sample (see Fig. 5) shows a small differences between $\Delta H_R = f(T)$ dependences in X and Q - bands and furthermore at high temperatures there is a tendency of reduction of this difference. This tendency gives support to the possibility that the internal field have a predominant contribution to the observed shift.

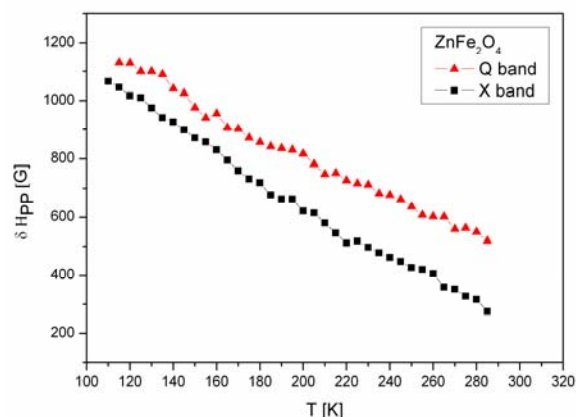


Fig. 6 Temperature dependences of the EPR line width, ΔH_{pp} , in: X- band and Q-band

Our measurements in X and Q - bands show that the resonance fields in Q-band are shifted by a factor which is equal with the frequency ratio. This behavior could point out to the absence of the ferromagnetic fluctuations in the investigated temperature range [23].

In the following, we discuss the temperature dependences in X and Q - bands of the EPR line width, ΔH_{pp} , for ZnFe₂O₄ sample which are presented in Fig. 6. These plots show in both bands an increase in the line width with decreasing temperature, the feature which is characteristic of superparamagnetic nanoparticles [21]. The evidenced temperature dependence of ΔH_{pp} implies the existence of a wide distribution of the exchange interactions between Fe³⁺ ions in ZnFe₂O₄ [10].

4. Conclusions

We have investigated by electron paramagnetic resonance (EPR) in X and Q - bands the nature of the magnetic interactions present in ZnFe₂O₄ nanoparticles. EPR spectrum consists of a single quite broad line which arises from exchange interactions between the Fe³⁺ ions. In X-band the line has a slightly asymmetrical line shape while in Q-band, the line shape is symmetric.

The presence of the superparamagnetic state in ZnFe₂O₄ samples was inferred from the VSM measurements and sustained by the analysis of the temperature behavior of EPR spectra. In the investigated temperature range and both X and Q - bands, a shift of the magnetic field position of the line to the lower field and a line broadening as the temperature is lowered were

observed. These features are the signature for the presence of the superparamagnetic state in our ZnFe₂O₄ nanoparticles. We have attributed the shift of the resonance field at X and Q - bands to the presence of a local field at the Fe³⁺ site due to the surrounding spin sublattice.

The observed line broadening could be due to the spin-glass freezing of the particle surface layer and indicates the existence of a wide distribution of the exchange interactions between Fe³⁺ ions in ZnFe₂O₄.

Acknowledgments

This work was supported by CNCSIS-UEFISCSU, project number PNII-IDEI Nr.4/2010, code ID-106.

References

- [1] T. Sato, K. Haneda, M. Seki T Iijima, Particles. Appl.Phys. A **50**, 13 (1990).
- [2] V. Blanco-Gutiérrez, M.J. Torralvo1, R. Sáez-Puche, P. Bonville, J. Phys.: Conference Series **200**, 072013 (2010).
- [3] H. Yang, X Zhang, C. Huang, W. Yang, G. Qiu, J. Phys, Chem. Solids **65**, 1329 (2004).
- [4] M. Sultan, R. Singh, J.Appl.Phys. **105**, 07A51 (2009).
- [5] S. Nakashima, K. Fujita, K. Tanaka, K. Hirao, J. Phys. Condens. Matter. **17**, 137 (2005) .
- [6] S. Popescu, P. Vlazan, S. Novaconi, I. Grozescu, P.V. Notingher, U.P.B. Sci. Bull. Series, **C 73** 247 (2011) .
- [7] A.T. Raghavender, Mater. Lett. **65**, 3636 (2011).
- [8] Y.F. Chen, D. Spoddig, M. Ziese, J.Appl.Phys. D **41**, 205004(2008).
- [9] S. Ayyappan, R.S. Philip, C. Venkateswaran, J. Philip, Appl.Phys.Lett. **96**, 143106- (2010).
- [10] M. Sultan, R. Singh, J. Phys: Conference Series **200**, 072090 (2010)
- [11] J.F. Hocheplied, M.P. Pileni J.Magn.Magn.Mat. **231**, 45 (2001).
- [12] D. Sibera, U. Narkiewicz, N. Guskos, G. Żolnierkiewicz, J Phys: Conference Series **146**, 012014 (2009).
- [13] H. Liu, J. Yang, Y. Zhang, Y. Wang, M. Wei, Mat. Chem.and Phys. **112**, 1021 (2008).
- [14] X.C. Wanga, W.B. Mi, D.F. Kuang, Appl. Surf. Sci. **256**, 1930 (2010).
- [15] J.H. Shim, T. Hwang, S. Lee, J.H. Park, S.J. Han, Y.H. Jeong Appl.Phys.Lett. **86**, 082503 (2005).
- [16] D. Karmakar, S.K. Mandal, R.M. Kadam, P.L. Paulose, A.K. Rajarajan, T.K. Nath, A.K. Das, I. Dasgupta, G.P. Das, Phys. Rev. B **75**, 144404 (2007).
- [17] O. Raita, A. Popa, M. Stan, R.C. Suciuc, A. Biris, L.M. Giurgiu Appl. Magn. Reson. **42**,499 (2012).
- [18] L. Yongbo, R. Yi, A. Yan, L. Deng, K. Zhou, X. Liu, Solid State Sci. **11**, 1319 (2009).

- [19] Y. A. Koksharov, S.P. Gubin, I.D. Kosobudsky, G.Y. Yurkov, D.A. Pankratov, L.A. Ponomarenko, M.G. Mikheev, M. Beltran, Y. Khodorkovsky, A.M. Tishin Phys. Rev. B **63**, 12407 (2000).
- [20] J. Kliava, S.P. Gubin Magnetic Nanoparticles, Willey-WCH, New York, (2009).
- [21] C. Oliva, L. Forni, Appl. Magn. Reson. **20**, 531 (2001).
- [22] A.D. McCarty, A.K. Hassan, L.C. Brune, K. Dziatkowski, J.K. Furdyna, Phys. Rev. Lett. **95**, 157201 (2005).
- [23] N. Poirot, P. Simon, P. Odier, Solid State Sci **10**, 186 (2008).
- [24] K. Kamazawa, Y. Tsunoda, H. Kadowaki, K. Kohn Phys. Rev. B **68**, 024412 (2003).

*Corresponding author: popa@itim-cj.ro